

Received April 23, 2020; reviewed; accepted August 16, 2020

## Effect of manganese ions addition orders on the flotation behavior of scheelite

Kuanwei Lu <sup>1</sup>, Rong Chen <sup>3</sup>, Ying Zhang <sup>1,2</sup>, Hongying Luo <sup>1</sup>, Hu Yang <sup>1</sup>, Jiaozhong Cai <sup>1</sup>

<sup>1</sup> Faculty of Land Resource Engineering, Kunming University of Science and Technology, Kunming 650093, China

<sup>2</sup> State Key Laboratory of Complex Nonferrous Metal Resources Clean Utilization, Kunming 650093, China

<sup>3</sup> The comprehensive utilization of resources in Xinyu Xingang Technology Co. Ltd

Corresponding author: zhyingcsu@163.com (Ying Zhang)

**Abstract:** In this study, the effect of  $MnCl_2$  on scheelite flotation with sodium oleate (NaOL) as a collector and sodium silicate as a depressant was assessed by a combination of flotation experiments, Fourier-transform infrared spectroscopy (FTIR), X-ray photoelectron spectroscopy (XPS), and solution chemistry. The flotation experiments confirmed that the addition of  $MnCl_2$  before sodium silicate showed an adverse effect on flotation and the recovery of scheelite gradually decreased as the amount of  $MnCl_2$  was increased. When  $MnCl_2$  was added after sodium silicate, the recovery of scheelite gradually increased with an increase in the amount of  $MnCl_2$ . The results of FTIR, XPS, and solution chemistry indicated that  $MnCl_2$  acted on the surface of scheelite in the form of manganese ions. When  $MnCl_2$  was added before sodium silicate, manganese ions adsorbed on the surface of scheelite reacted with sodium silicate to form a hydrophilic silicate, which covers the surface of scheelite and blocks the adsorption of NaOL. However, when  $MnCl_2$  was added after sodium silicate, manganese ions are continued to be adsorbed on the surface of scheelite, which increases the cations on the surface of scheelite, and hence the condition becomes conducive for the interaction between scheelite and NaOL.

**Keywords:** manganese ion, addition order, scheelite, sodium silicate, flotation

### 1. Introduction

Tungsten, as a global strategic resource, is widely used in many fields such as machinery, electricity, metallurgy, chemistry, etc. (Kupka et al., 2018; Dong et al., 2019a). Currently, the main minerals that are used to extract tungsten metals are wolframite and scheelite (Wang et al., 2018; Dong et al., 2019b). Scheelite, as a main tungsten-containing mineral (Gao et al., 2015), is generally separated from its gangue minerals by flotation (Hu et al., 2012; Yin and Wang, 2014; Bo et al., 2015; Gao et al., 2016; Zhang et al., 2017). The commonly used collectors for scheelite flotation are fatty acids and fatty acid derivatives (Filippova et al., 2018), among them sodium oleate (NaOL) is the most common. This kind of collector primarily collects scheelite by chemical adsorption between oleate ion and mineral surface (Ignatkina, 2017). Therefore, it is difficult to effectively separate scheelite from calcium-containing gangue minerals with fatty acid collectors without the use of a depressant (Li et al., 1983).

Depressants are typically used to depress the floatability of gangue minerals during the scheelite flotation process. Inhibitors are mainly organic inhibitors such as dextran sulfate (Chen et al., 2017), xanthan gum (Dong et al., 2019), and carboxyl methylcellulose (Wang et al., 2018), and inorganic inhibitors such as sodium fluorosilicate (Dong et al., 2019) and sodium phosphates (Li and Li, 1983), etc. However, they exhibit either a relatively weak depression effect on gangue minerals or undesirable depression effects on scheelite. Therefore, sodium silicate remains the most commonly used depressant in industrial scheelite flotation. Sodium silicate is widely used in scheelite flotation due to its good depression on calcium-containing minerals, relatively good selectivity, high efficiency, and low cost (Marinakakis and Shergold, 1985; Sun et al., 2013; Zhang et al., 2014; Cheng et al., 2016).

Also, a large number of studies have shown that the addition of some metal ions such as  $\text{Pb}^{2+}$ ,  $\text{Fe}^{2+}$ ,  $\text{Al}^{3+}$ ,  $\text{Fe}^{3+}$ , etc., can effectively improve the flotation separation of scheelite and calcium-containing gangue minerals (Deng et al., 2018; Tian et al., 2018; Zhao et al., 2018; Wang et al., 2019; Yao et al., 2020). These metal ions are primarily adsorbed on the scheelite surface in the form of cations which increase the active sites on the scheelite surface (Zhao et al., 2015). These metal ions can also adsorb on the surface of calcium-containing gangue minerals after acting on the depressant, which enhances the depression on calcium-containing gangue minerals. Therefore, the flotation and separation of scheelite are improved (Feng et al., 2016). Although these metal ions have a good separation effect from the calcium-bearing gangue minerals, scheelite is also associated with wolframite in deposits, wolframite dissolve of iron, and manganese ions in the pulp, the existence of two kinds of metal ions can affect the scheelite selecting index.

In our previous studies, it was found that the effect of manganese ions on scheelite was interesting (Chen et al., 2016, 2017, 2018; Chen, 2019). Therefore, this study was aimed to investigate the effect of manganese ions on the scheelite flotation behavior. Additionally, the previous studies have mainly focused on the selectivity of metal ions and depressant mixture on minerals, and ignored the addition order of metal ions and depressants. Underestimating the importance of addition order in the flotation plant may result in different flotation behaviors of minerals and potential recovery loss.

For this purpose,  $\text{MnCl}_2$  was used to obtain as a source of  $\text{Mn}^{2+}$ , NaOL was used as a collector, and sodium silicate was used as a depressant. Additionally, the influence of the addition order of  $\text{Mn}^{2+}$  on scheelite flotation was studied by adjusting the addition order of  $\text{MnCl}_2$ . The adsorption of  $\text{MnCl}_2$  on the surface of scheelite, and the influence of  $\text{Mn}^{2+}$  on the adsorption of NaOL and sodium silicate on the surface of minerals were further studied by using solution chemical calculation, Fourier-transform infrared spectroscopy (FTIR) and X-ray photoelectron spectroscopy (XPS) analyses. The potential reaction mechanism was established to further understand the influence of  $\text{Mn}^{2+}$  on the selectivity of sodium silicate and the action mechanism on the scheelite surface.

## 2. Materials and methods

### 2.1. Materials

The scheelite sample used for all experiments was obtained from Tongde County Kumuda Mining Co., Ltd., in Qinghai Province, China. The sample was selected by hand, crushed by a ceramic jaw crusher, and ground by a three-head grinding machine to collect the  $-75+38 \mu\text{m}$  for the micro-flotation experiments. The samples with a particle size of less than  $38 \mu\text{m}$  were further ground to below  $5 \mu\text{m}$  for X-ray diffraction (XRD), FTIR, and XPS analyses. The XRD and chemical analyses of the scheelite sample are shown in Fig. 1 and Table 1, respectively.

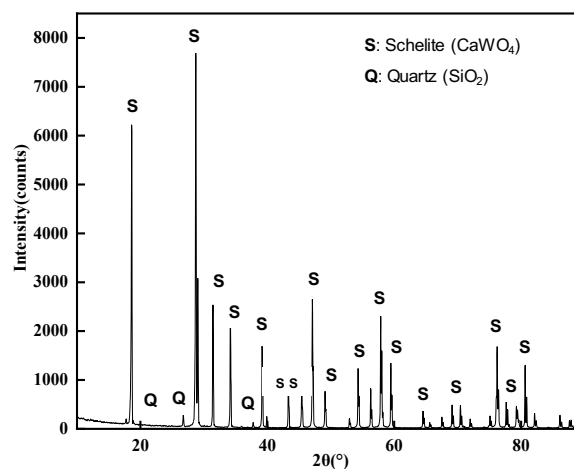


Fig. 1. XRD analysis of scheelite sample

As seen from Fig. 1, the sample contained mainly scheelite and minor quartz particles. As indicated in Table 1 that the purity of  $\text{WO}_3$  was 75.44%. The reagents used in the experiment primarily included

Table 1. Chemical composition of scheelite sample

Compound	CaO	WO <sub>3</sub>	SiO <sub>2</sub>
Content (%)	18.16	75.44	6.40

NaOL (analytical pure, Tianjin Guangfu Fine Chemical Research Institute), sodium silicate (analytical pure, Tianjin Chemical Reagent Technology Co., Ltd.), and manganese chloride (analytical pure, Chengdu Kelon Chemical Reagent Factory). HCl and NaCO<sub>3</sub> were used as pH regulators. Deionized (DI) water with a resistivity of 18.25 MΩ × cm was used for all experiments.

## 2.2. Flotation experiments

The flotation experiments were carried out using an XFG flotation machine with a stirring speed of 1650 r/min in a 40 cm<sup>3</sup> plexiglass cell. The experiments were performed in the following order (Fig. 2): Firstly, 35 cm<sup>3</sup> of DI water was added to the flotation cell and 3.0 g of pure mineral, the flotation cell was fixed on the flotation machine, the suspension was stirred for 1 min, and then HCl or NaOH was added to adjust the pH of the suspension. Then, the suspension was stirred for another 2 min, and then the pH of the suspension was measured and recorded. The flotation reagents were then added every 3 min in order; the froth collection time was 4 min; the float and sink products were collected, filtered, and dried. Finally, the recovery of minerals was calculated by their dry weights. The experiments were repeated three times, and the average values were calculated.

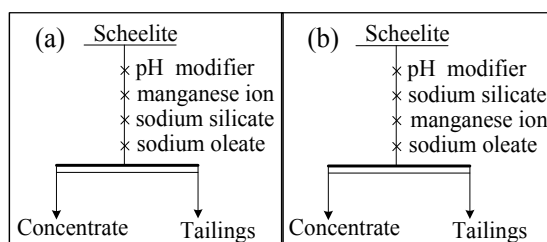


Fig. 2. Flowsheet of the flotation experiment

## 2.3. Fourier-transform infrared spectroscopy (FTIR) analysis

The Nicolet FTIR-740 Fourier transform infrared spectrometer was used for detection in the wavenumber range of 4000–400 cm<sup>-1</sup>. The preparation process of the mineral sample by using FTIR analysis was as follows: 1 g of the mineral sample (–5 μm) was dispersed in 40 cm<sup>3</sup> of DI water. Then, the pH of the slurry was adjusted, and an appropriate dose of the flotation reagent was added. After stirring for 30 min on a magnetic stirrer, it was repeatedly washed with DI water of the same pH and suction filtered by using a microporous membrane. The samples were dried at a constant temperature (40°C) in a vacuum oven. The dried samples and KBr powder were ground and mixed in the agate mortar, and then pressed into pieces in a tablet pressing machine and used for the FTIR analysis.

## 2.4. X-ray photoelectron spectroscopy (XPS) analysis

The PHI5000 Versaprobe-II multifunctional scan imaging photoelectron spectroscopy was used for XPS analysis. The sample used for XPS detection had the same particle size and reagent system as the flotation process. The sample was filtered and washed repeatedly with DI water for washing away the weak physical adhesion of the reagent on the mineral surface. Then, it was dried in a vacuum oven (40°C) and used for the XPS analysis.

## 3. Results and discussion

### 3.1. Effect of MnCl<sub>2</sub> on the scheelite flotation using sodium silicate and NaOL

The effect of the NaOL concentration on the flotation recovery of scheelite is shown in Fig. 3. As seen in Fig. 3, the recovery of scheelite constantly increases with an increase in NaOL concentration. When the concentration of NaOL is 5×10<sup>-4</sup> mol/dm<sup>3</sup>, the recovery of scheelite is found to be 87%, the amount of

NaOL continues to increase, and the recovery increases gradually. Therefore, in the subsequent flotation experiments, the NaOL concentration was chosen as  $5 \times 10^{-4}$  mol/dm<sup>3</sup>.

The effect of the pulp pH on the flotation recovery of scheelite is shown in Fig. 4. As the pH of the slurry increases, the recovery of scheelite continuously increases. At a pH of about 9, the recovery of scheelite reaches the maximum value (87%), the pH of the pulp continues to increase, and the recovery of scheelite begins to decrease. Therefore, the optimum pH value of scheelite flotation was determined to be about 9.

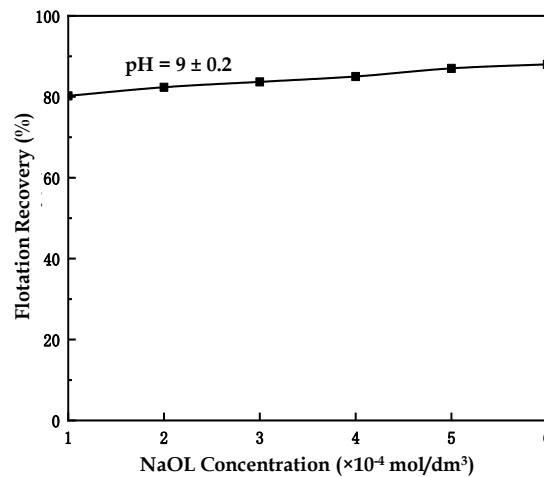


Fig. 3. Effect of the NaOL concentration on the flotation recovery of scheelite

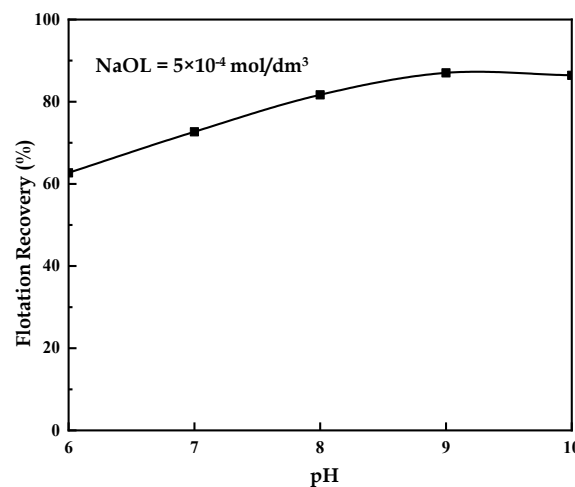


Fig. 4. Effect of the pulp pH on the flotation recovery of scheelite

The effect of the sodium silicate concentration on the flotation recovery of scheelite is shown in Fig. 5. As the concentration of sodium silicate increases, the recovery of scheelite continuously decreases, which indicates that sodium silicate exhibits a certain depression on scheelite flotation.

The influence of the addition order of Mn<sup>2+</sup> and the concentration on the flotation recovery of scheelite is shown in Fig. 6. Firstly, in Fig. 6(a), with an increase in the concentration of Mn<sup>2+</sup>, the recovery of scheelite increases. When the concentration of Mn<sup>2+</sup> is  $5 \times 10^{-4}$  mol/dm<sup>3</sup>, the recovery is found to be 89%, i.e., 2.63% higher than the recovery rate of scheelite in the NaOL system, which indicates that this addition order improves the interaction between NaOL and scheelite, thus a better flotation recovery is obtained. However, compared to Fig. 5 (in the case of scheelite + sodium silicate + NaOL), Mn<sup>2+</sup> was added after of sodium silicate, the recovery of scheelite increased instead of decreasing, which indicated that Mn<sup>2+</sup> not only weakened the depression of scheelite by sodium silicate but also played a major role in the activation of scheelite. Secondly, in Fig. 6(b), compared to the flotation system without Mn<sup>2+</sup> (Figs. 3 and 4), with an increase in the concentration of Mn<sup>2+</sup>, the flotation recovery

of scheelite decreases, which shows that the depression of  $\text{Mn}^{2+}$  on the flotation of scheelite is more obvious. In other words, the addition of  $\text{Mn}^{2+}$  strengthens the depression of scheelite flotation by using sodium silicate, which is similar to that of salinized sodium silicate, and it is speculated that it may have the same depression mechanism as salinized sodium silicate.

The results for the flotation experiments show that when the pH value of the pulp is about 9, sodium silicate shows a depression effect on scheelite. Adding  $\text{Mn}^{2+}$  before sodium silicate can enhance the depression of scheelite by sodium silicate, and it is found to be similar to the salinized sodium silicate. However, when  $\text{Mn}^{2+}$  was added after NaOL, it not only makes scheelite undepressed by using sodium silicate but also plays a major role in the activation of scheelite. When the concentration of NaOL was  $5 \times 10^{-4} \text{ mol/dm}^3$ , the concentration of sodium silicate was  $2 \text{ g/dm}^3$  and the concentration of  $\text{Mn}^{2+}$  was  $5 \times 10^{-4} \text{ mol/dm}^3$ . The recovery of scheelite obtained from the two addition orders was differed by 54.18%, this shows that the addition order of  $\text{Mn}^{2+}$  influenced the flotation of tungsten minerals to a large extent.

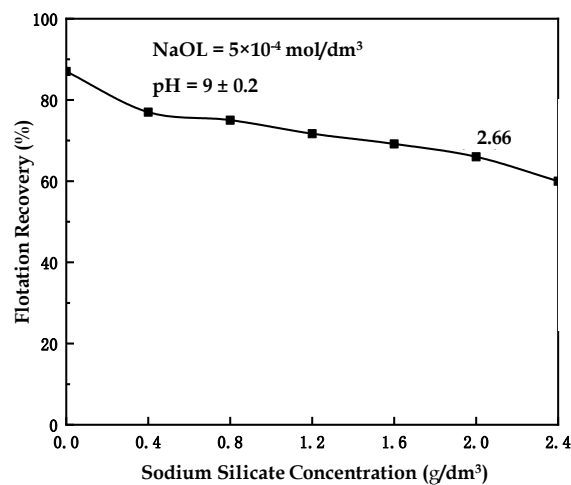


Fig. 5. Effect of the sodium silicate concentration on the flotation recovery of scheelite

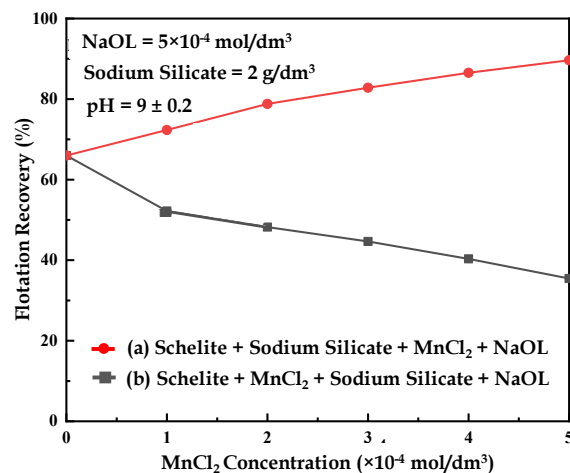


Fig. 6. Effect of the addition order and dosage of manganese ions on the flotation behavior of scheelite

### 3.2. FTIR analysis

The infrared spectrum of NaOL is shown in Fig. 7. The symmetric vibration peak of  $-\text{C}-\text{H}$  in scheelite appeared at  $2922.24 \text{ cm}^{-1}$  (Chen et al., 2018). The peaks at  $1560.61 \text{ cm}^{-1}$  and  $1451 \text{ cm}^{-1}$  were contributed by the symmetric vibration peak of  $-\text{COO}-$  (Espiritu et al., 2018). The characteristic peaks at  $923.60 \text{ cm}^{-1}$  were assigned to the symmetrical telescopic peak of  $-\text{C}-\text{O}-\text{C}-$ .

The infrared spectrum of scheelite under different conditions is shown in Fig. 8. The peaks at  $811.27$

$\text{cm}^{-1}$  and  $439.45 \text{ cm}^{-1}$  were contributed by asymmetric stretching vibration peaks and out-of-plane bending vibration absorption peaks of  $-\text{W}-\text{O}$  bonds of  $\text{WO}_4^{2-}$ . After the interaction with NaOL, the antisymmetric stretching peak of  $-\text{C}-\text{H}$  appeared at  $2924.71 \text{ cm}^{-1}$  and the peaks that appeared at  $1637.26 \text{ cm}^{-1}$  and  $1403.19 \text{ cm}^{-1}$  were contributed by the vibration  $-\text{COO}-$ , indicating that the chemical adsorption or the reaction of NaOL on the surface of scheelite occurred, which was found to be consistent with the flotation results.

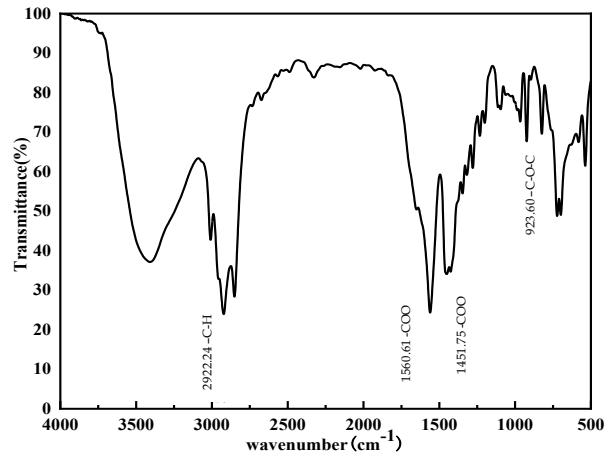


Fig. 7. Infrared spectrum of NaOL

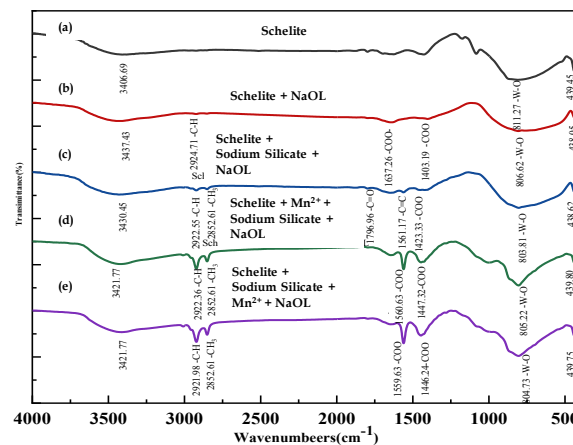


Fig. 8. The infrared spectrum of scheelite under different conditions

After the interaction of scheelite with NaOL and sodium silicate, the surface of scheelite exhibits a symmetric stretching peak of  $-\text{CH}_3$  at  $2852.07 \text{ cm}^{-1}$ , and the peak is observed to be strong and two stretching vibrations of  $\text{C}=\text{O}$  are found to be coupled. A vibrational stretching peak of  $\text{C}=\text{O}$  appeared at  $1796.96 \text{ cm}^{-1}$ , a stretching peak of  $\text{C}=\text{C}$  appeared at  $1561.17 \text{ cm}^{-1}$ , and a symmetric stretching peak of  $-\text{COO}-$  appeared at  $1423.33 \text{ cm}^{-1}$ . From these peaks, it can be inferred that after the action of scheelite with NaOL, the surface of scheelite changed significantly, and chemical adsorption or surface reaction occurred between the NaOL and scheelite.

In the infrared spectra of scheelite, when sodium silicate and  $\text{Mn}^{2+}$  were added, it can be seen that no matter if  $\text{Mn}^{2+}$  was added after or before the sodium silicate, the surface of scheelite the symmetric vibration peak of  $-\text{C}-\text{H}$  at  $2922.36 \text{ cm}^{-1}$  and  $2921.98 \text{ cm}^{-1}$ , a stretching peak of  $-\text{COO}$  at  $1560.63 \text{ cm}^{-1}$ , and an asymmetric angular vibration absorption peak of  $-\text{COO}$  at  $1446.24 \text{ cm}^{-1}$ . These peaks also appeared when conventional agents were added, but their strength was found to be stronger than that of scheelite untreated with manganese ions. Comparing the infrared spectrum of different addition orders of  $\text{Mn}^{2+}$ , it is observed that the peak formed by the addition of  $\text{Mn}^{2+}$  after the sodium silicate was stronger, which indicates that  $\text{Mn}^{2+}$  can increase the adsorption of NaOL on the mineral surface, but as manganese silicate covers the surface of scheelite and the flotation effect is poor. It also shows that the addition of

Mn<sup>2+</sup> after the sodium silicate can increase the adsorption of the agent on the surface of scheelite, consistent with the flotation result.

### 3.3. XPS analysis

The XPS analysis was conducted to study the action mechanism of the addition order of Mn<sup>2+</sup> on the scheelite surface. XPS narrow-edge scanning was used to analyze O elements of different shapes on the scheelite surface, and the results are shown in Table 2.

Table 2. The ratio of binding energy and the atomic concentration of O1s on the scheelite surface

Samples	Binding energy (eV)	Status	Area ratio (%)
Scheelite + sodium silicate + NaOL	530.32	-W-O	29.71
	531.26	-COO-	37.95
	532.41	-Si-O	24.29
	533.33	-OH	8.04
Scheelite + Mn <sup>2+</sup> + Sodium silicate + NaOL	530.45	-W-O	31.46
	531.24	-COO-	23.57
	532.25	-Si-O	36.57
	533.16	-OH	8.60
Scheelite + Sodium Silicate + Mn <sup>2+</sup> + NaOL	530.35	-W-O	35.62
	531.40	-COO-	39.92
	532.42	-Si-O	15.32
	533.16	-OH	9.14

The XPS spectrum of Mn2p on the surface of scheelite after different addition orders is shown in Fig. 9. The characteristic peaks of manganese on the surface of scheelite can be detected under both conditions, which indicates that manganese is adsorbed on the surface of scheelite and metal salts of manganese are formed. Besides, in Fig. 10 (a) and (b), the binding energies of Mn2p are 642.05 eV and 642.21 eV, respectively, which may be caused by Mn-O (Yang et al., 2015). The reason is that manganese ions are added to scheelite to form manganese oxides.

The XPS energy spectrum of O1s on the surface of scheelite under different conditions is shown in Fig. 11. The XPS spectrum of O1s on the surface of scheelite treated with NaOL and sodium silicate is shown in Fig. 11(a). The binding energies of O in -W-O, -COO-, -Si-O, and -OH are 530.32 eV, 531.26 eV, 532.41 eV, and 533.33 eV, respectively (Tian et al., 2018; Wang et al., 2018; Zhao et al., 2018; Dong et al., 2019a; Wei et al., 2020). The XPS spectrum of O1s on the surface of scheelite treated with Mn<sup>2+</sup>, sodium silicate, and NaOL is shown in Fig. 11(b). The binding energies of O in -W-O, -COO-, -Si-O, and -OH (Wang et al., 2020) are 530.45 eV, 531.24 eV, 532.25 eV, and 533.16 eV, respectively. The XPS spectrum of O1s on the surface of scheelite treated with sodium silicate, Mn<sup>2+</sup>, and NaOL is shown in

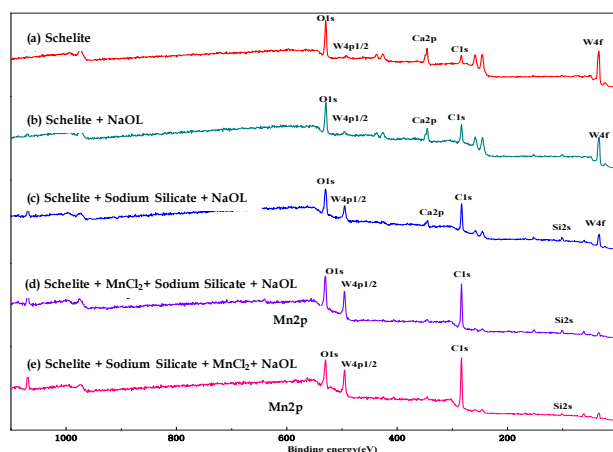


Fig. 9. XPS energy spectrum of the scheelite surface with different reagents

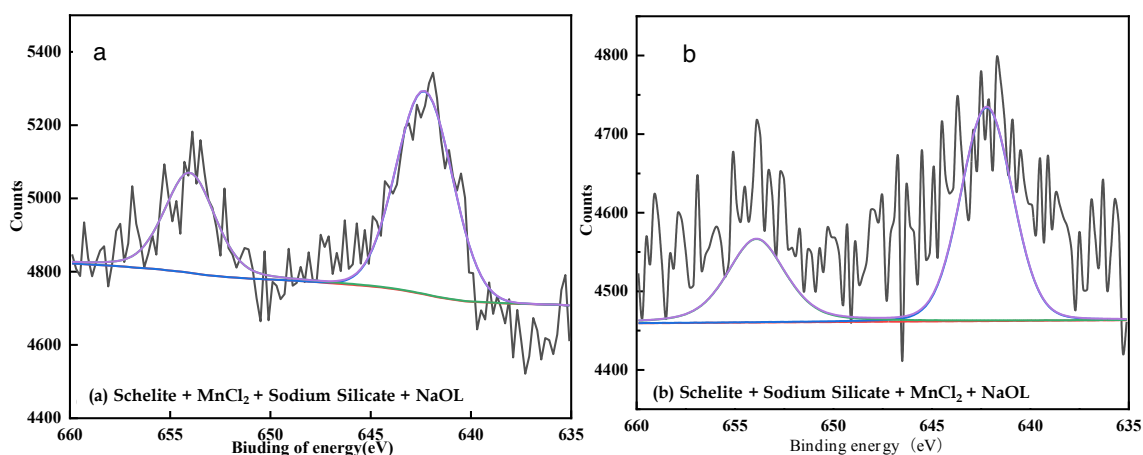


Fig. 10. The XPS spectrum of Mn2p on the surface of scheelite under various conditions: (a) Scheelite + MnCl<sub>2</sub> + sodium silicate + NaOL (b) Scheelite + sodium silicate + MnCl<sub>2</sub> + NaOL

Fig. 11(c). The binding energies of O in -W-O, -COO-, -Si-O, and -OH are 530.45 eV, 531.40 eV, 532.42 eV, and 533.16 eV, respectively. The existence of -W-O due to WO<sub>4</sub><sup>2-</sup> and -COO- may be caused by the adsorption of NaOL on the surface of scheelite, whereas the existence of Si-O is caused by silicate ions reacting with metal ions on the surface of scheelite and resulting in silicate precipitation. The appearance of -OH is attributed to the hydroxyl precipitation formed by the action of dissolving metal ions and -OH in water.

It can be seen from Figs. 11(a) and (b), and the flotation results that scheelite is depressed without Mn<sup>2+</sup> and by adding Mn<sup>2+</sup> before sodium silicate. In Table 2, it can be seen that the content of O in -Si-O is greater than that of -Si-O without Mn<sup>2+</sup>. This may be because Mn<sup>2+</sup> is adsorbed on the surface of scheelite reacts with silicate root for generating more silicates. The content of O in -COO- decreases, indicating that silicate precipitation increases and covers the surface of scheelite, and thus the adsorption of NaOL on the surface of scheelite was hindered. It can be seen from Figs. 11(a) and (c), and Table 2 that the content of -COO- has increased and the content of Si-O has decreased. When sodium silicate is added, it reacts with Ca<sup>2+</sup> on the surface of scheelite to form calcium silicate. During this period, WO<sub>4</sub><sup>2-</sup> on the surface of scheelite is considered to be the dominant component. Then, MnCl<sub>2</sub> is added, and Mn<sup>2+</sup> is still adsorbed on the surface of scheelite, which shows a certain activation effect on scheelite. While comparing Figs. 11(b) and (c), the addition order of MnCl<sub>2</sub> is different, and the XPS spectrum of O1s on the surface of scheelite is also different. The content of O in -Si-O and -COO- shows the most significant changes with 21.25% and 16.35%, respectively. The primary reason is that the different addition orders of reagents lead to different priorities. The results of the above analysis are observed to be consistent with the flotation results and FTIR analysis.

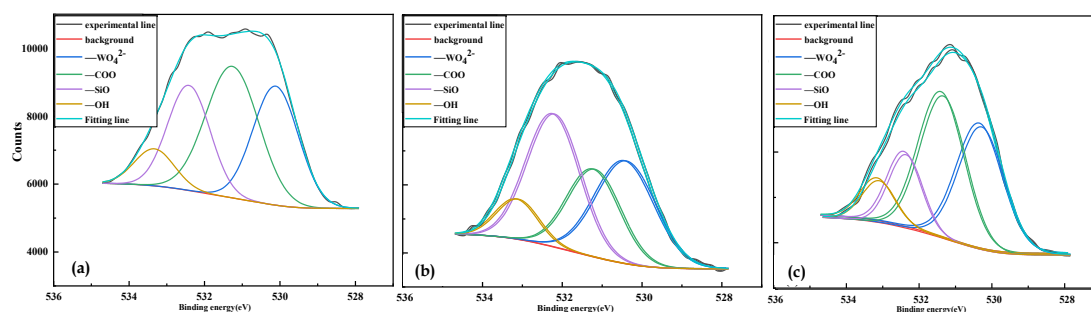


Fig. 11. The XPS energy spectrum of O1s on the surface of scheelite under different conditions: (a) Scheelite + sodium silicate + NaOL (b) Scheelite + MnCl<sub>2</sub> + sodium silicate + NaOL (c) Scheelite + sodium silicate + MnCl<sub>2</sub> + NaOL

#### 4. Solution chemical analysis and discussion

Solution chemical analysis is useful in determining the mechanism of action between minerals and

agents. In particular, this analysis can be used to analyze the existing forms of minerals or agents at a specific pH and the possible reaction mechanism.

Scheelite is a kind of oxidation ore with less floatability than sulfide ore, and a dissolution phenomenon is observed in water. The solution composition of scheelite is shown in Fig. 12. When  $\text{pH} < 4.7$ , the solution composition primarily includes  $\text{Ca}^{2+}$ ,  $\text{H}_2\text{WO}_4$ , and  $\text{WO}_4^{2-}$ ; when  $\text{pH} = 4.7$  to 13.71, the solution composition primarily includes  $\text{Ca}^{2+}$ ,  $\text{WO}_4^{2-}$ ,  $\text{HWO}_4^-$ , and  $\text{Ca}(\text{OH})^+$ . When scheelite dissolves in water,  $\text{Ca}^{2+}$  dissociates better than  $\text{WO}_4^{2-}$ , which causes excess negative charge on the surface of scheelite. When the optimal pH of the flotation is about 9,  $\text{WO}_4^{2-}$  and  $\text{Ca}^{2+}$  are considered the dominant species in the solution.

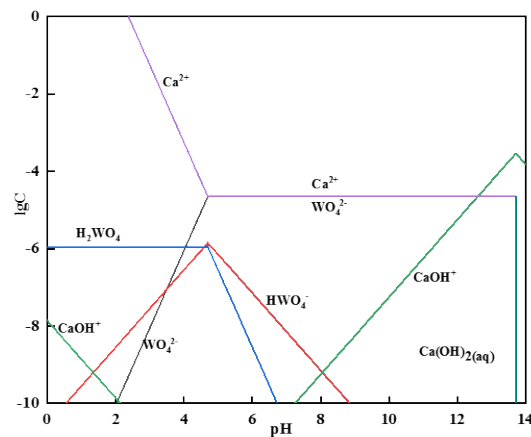


Fig. 12. The solution composition of the scheelite

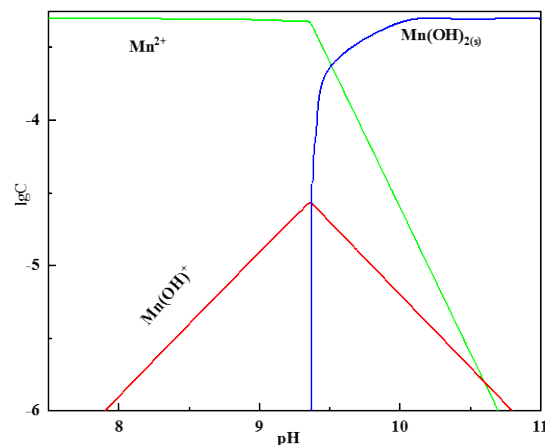
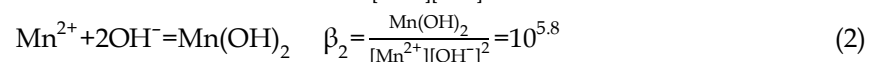
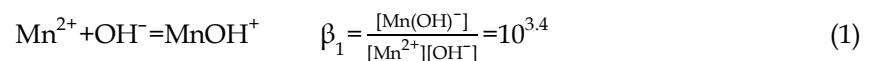


Fig. 13. Species distribution diagram of  $5 \times 10^{-4} \text{ mol/dm}^3 \text{ Mn}^{2+}$  as a function of pH values

To study the existing form of manganese ions on the mineral surface, the relationship between the dissolved components of  $\text{Mn}^{2+}$  in the solution and pH was calculated, where the concentration of manganese ions was found to be  $5 \times 10^{-4} \text{ mol/dm}^3$ . The relative reactions used in the calculation are as follows:



$$[\text{M}]' = [\text{Mn}^{2+}] + [\text{MnOH}^+] + [\text{Mn}(\text{OH})_2] = [\text{Mn}^{2+}](1 + \beta_1[\text{OH}^-] + \beta_2[\text{OH}^-]^2) \quad \alpha_M = \frac{[\text{M}]'}{[\text{Mn}^{2+}]} = (1 + \beta_1[\text{OH}^-] + \beta_2[\text{OH}^-]^2) \quad (3)$$

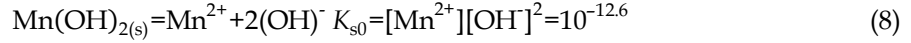
$$[\text{Mn}^{2+}] = \frac{[\text{M}]'}{\alpha_M} = \frac{[\text{M}]'}{1 + \beta_1[\text{OH}^-] + \beta_2[\text{OH}^-]^2} \quad (4)$$

$$\log[\text{Mn}^{2+}] = \log[\text{M}]' - \log(1 + \beta_1[\text{OH}^-] + \beta_2[\text{OH}^-]^2) \quad (5)$$

$$\log[\text{Mn}(\text{OH})^+] = \log\beta_1 + \log[\text{Mn}^{2+}] + \log[\text{OH}^-] \quad (6)$$

$$\log[\text{Mn}(\text{OH})_2] = \log\beta_2 + \log[\text{Mn}^{2+}] + 2\log[\text{OH}^-] \quad (7)$$

In general, three types of manganese-containing substances can be found in aqueous solutions containing manganese ions:  $\text{Mn}^{2+}$ ,  $\text{Mn}(\text{OH})_{2(s)}$ , and  $\text{Mn}(\text{OH})^+$ . Their corresponding chemical reactions and equilibrium constants are shown in the following equations:



The concentration of each component:

$$\log[\text{Mn}^{2+}] = \log K_{s0} - 2\log[\text{OH}^-] \quad (10)$$

$$\log[\text{Mn}(\text{OH})^+] = \log K_{s1} - \log[\text{OH}^-] \quad (11)$$

Based on the above deductions, the distribution coefficients of various manganese-containing complexes can be calculated as a function of pH values. The resulting relationships are shown in Fig. 13. As shown in Fig. 13, the distributions of different manganese-containing complexes in the aqueous solution are closely related to the pH value of the solution. At pH values below 9.35, manganese in the aqueous solution primarily exists as dissociated  $\text{Mn}^{2+}$  and  $\text{Mn}(\text{OH})^+$ . At  $\text{pH} > 9.35$ , the content of  $\text{Mn}^{2+}$  and  $\text{Mn}(\text{OH})^+$  in the solution gradually decreases, and the precipitation of  $\text{Mn}(\text{OH})_2$  occurs. When the optimal pH value of flotation is about 9,  $\text{MnCl}_2$  is adsorbed on the surface of scheelite in the form of  $\text{Mn}^{2+}$  and  $\text{Mn}(\text{OH})^+$  (Sun et al., 2018).

The distribution coefficients of sodium silicate in aqueous solutions as a function of pH values are shown in Fig. 14.  $[\text{SiO}(\text{OH})_4]$ ,  $[\text{SiO}_2(\text{OH})_2^{2-}]$ , and  $[\text{SiO}(\text{OH})_3^-]$  (Zhang et al., 2019) all react with the scheelite surface. According to Figs. 3-7 and 11, the following conclusions can be drawn: scheelite is depressed only in the presence of sodium silicate.

The solution chemistry graph of NaOL is shown in Fig. 15. It shows that different types of species can be formed, such as  $\text{RCOOH}_{(l)}$ ,  $\text{RCOOH}_{(aq)}$ ,  $(\text{RCOO}^-)_2^{2-}$ ,  $\text{RCOO}^-$ , and  $\text{RCOO}^- \text{RCOO}^-$  (Wang et al., 2020). At  $\text{pH} < 8.68$ , undissociated acid is the main species and it starts to precipitate as the pH decreases, the concentration of  $(\text{RCOO}^-)_2^{2-}$  and  $\text{RCOO}^-$  increases, and the recovery of scheelite also increases gradually. At  $\text{pH} < 8.68$ ,  $(\text{RCOO}^-)_2^{2-}$  and  $\text{RCOO}^-$  reached saturation. During this period, the hydrolysis component of NaOL in the solution is mainly  $(\text{RCOO}^-)_2^{2-}$  and  $\text{RCOO}^-$ . Combined with the flotation test, it is observed that the main components of NaOL which affect flotation are  $(\text{RCOO}^-)_2^{2-}$  and  $\text{RCOO}^-$ .  $\text{Ca}^{2+}$  plays a major role on the surface of scheelite and the dominant component of manganese is  $\text{Mn}^{2+}$ . The flotation effect of the scheelite + sodium silicate +  $\text{MnCl}_2$  + NaOL flotation system is found to be better than that of scheelite +  $\text{MnCl}_2$  + sodium silicate + NaOL because  $\text{MnCl}_2$  increases the active site on the surface of scheelite and oleic acid; the dominant component of NaOL can react with it to allow the oleic acid dimer and oleate anion to be captured on the mineral surface, thereby increasing the flotation recovery of scheelite.

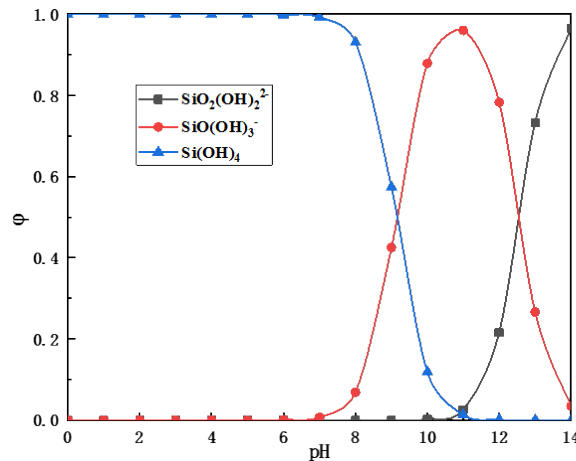


Fig. 14. Species distribution diagram of silicate as a function of pH

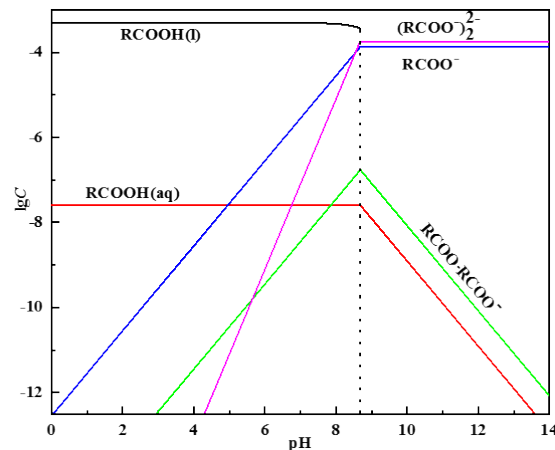


Fig. 15. Species distribution diagram of  $5 \times 10^{-4}$  mol/dm<sup>3</sup> NaOL as a function of pH

The reaction of NaOL and Mn<sup>2+</sup> can be monitored by standard Gibbs free energy changes ( $\Delta G^\theta$ ). Suppose NaOL reacts with Mn<sup>2+</sup> primarily in the form of oleate ions in the aqueous solution, and the reaction is expressed as follows:

The protonation reactions of HOL in water are expressed as follows:

As the reactions include side reactions, the coefficient of the side reaction is expressed as follows:

$$\alpha_{(OL)} = 1 + K^H [H^+] \quad (12)$$

$$\alpha_{Mn^{2+}} = 1 + \beta_1' [OH^-] + \beta_2' [OH^-]^2 + \beta_3' [OH^-]^3 + \beta_4' [OH^-]^4 \quad (13)$$

where  $Ls_{Mn(OL)_2}$  is the solubility product of  $Mn(OL)_2$ , and  $\beta_n$  and  $\beta_n'$  are the cumulative stability constants of Mn<sup>2+</sup>. The results are shown in Table 3.

Table 3. Stability constants of metal ion hydroxy complex (25°C)

Ion	lg $\beta_1$	lg $\beta_2$	lg $\beta_3$	lg $\beta_4$
Mn <sup>2+</sup>	3.4	5.8	7.2	7.3

$$\Delta G_{Mn^{2+}}^\theta = RT \ln Ls' = RT \ln (Ls_{Mn(OL)_2} \alpha_{Mn^{2+}} \alpha_{(OL)}^2) \quad (14)$$

where  $\Delta G_{Mn^{2+}}^\theta$  is Gibbs free energy,  $T$  is temperature,  $Ls_{Mn(OL)_2}$  is solubility product of  $Mn(OL)_2$  and  $R$  is the constant.

Substituting the relative parameters into the corresponding equations, we obtain:

$$\Delta G_{Mn^{2+}}^\theta = RT \ln \{ 10^{-15.3} \times [1 + 10^{pH-11.42} + 10^{2pH-27} + 10^{3pH-34.8} + 10^{4pH-48.7}] \times (1 + 10^{6-pH})^2 \} \quad (15)$$

The relative curve between the pH and  $\Delta G$  can be plotted as shown in Fig. 16. The  $\Delta G_{Mn^{2+}}^\theta$  is found to be negative in the pH range of 2-14. The results of the thermodynamic analysis showed that, indicating that the reaction between NaOL and Mn<sup>2+</sup> occurs spontaneously. Also, the solution is weakly alkaline, the value of  $\Delta G_{Mn^{2+}}^\theta$  reaches the most negative. That is to say, the flotation index of scheelite in Fig. 6(a) can reach the best when pH is 9. Because the thermodynamic calculation results negative of Mn<sup>2+</sup> and NaOL over a wide pH range, which makes it is possible for the added manganese ions to effectively increase the active site on the scheelite surface. XPS analysis also found Mn - containing material on scheelite surface of after manganese ion action. Therefore, the addition of manganese ions after sodium silicate eventually promotes the flotation of scheelite.

Based on the flotation tests, FTIR analysis, XPS, and the thermodynamic analysis result, the effect of Mn<sup>2+</sup> on the scheelite flotation using NaOL can be plotted as shown in Figs. 17 and 18.

In Figs. 17 and 18, when Mn<sup>2+</sup> is added first, it interacts with the surface of scheelite to form more active particles on the surface of scheelite. After adding sodium silicate, the newly added cations on the surface of scheelite are adsorbed with the silicate ions hydrolyzed by sodium silicate; consequently, the silicate ions react with these cation particles, thus form a hydrophilic silicate cover on the surface of

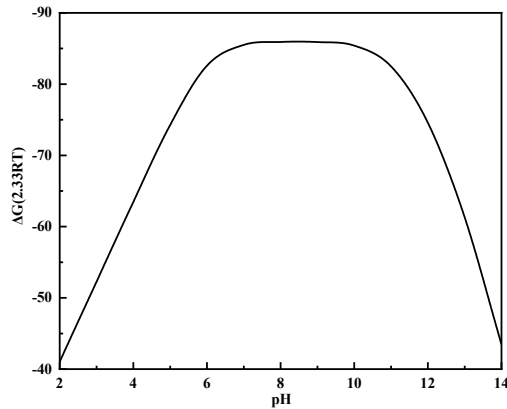


Fig. 16. Relationship between  $\Delta G$  and pH in the reaction of NaOL and  $Mn^{2+}$  ions

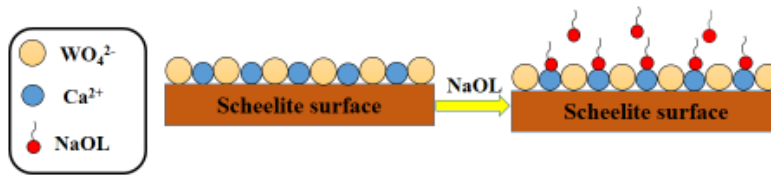


Fig. 17. Schematic diagram of the reaction between the scheelite surface and NaOL

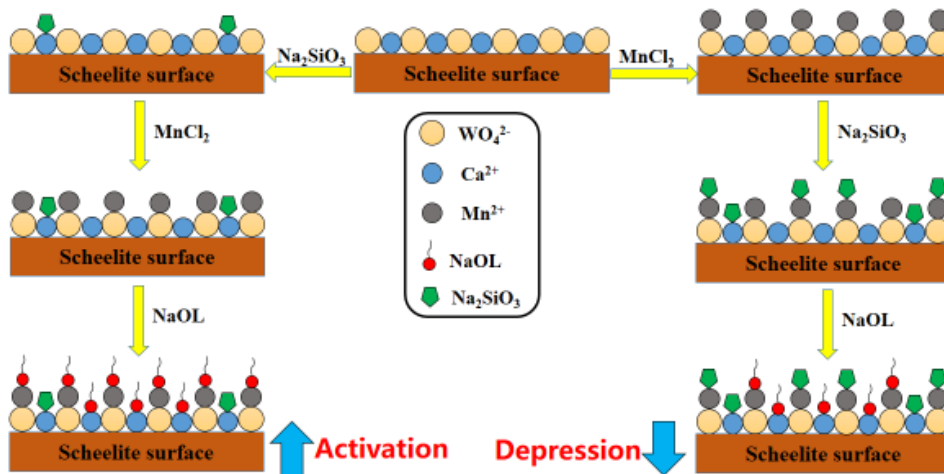


Fig. 18. Schematic diagram of the reaction between the scheelite surface and  $Mn^{2+}$

scheelite, hinder the adsorption of NaOL on the scheelite surface, and reduce the recovery of scheelite. The sodium silicate is first added to form silicate on the surface of scheelite, and then the added  $Mn^{2+}$  is still adsorbed on the surface of scheelite treated by the sodium silicate. When NaOL is added, both  $Mn^{2+}$  and  $Ca^{2+}$  on the surface of scheelite are adsorbed by NaOL, which helps in the activation of scheelite.

## 5. Conclusions

In this study, the effect and mechanism of the  $MnCl_2$  concentration and its addition order on the flotation behavior of scheelite are studied. Based on the flotation tests, FTIR analysis, XPS, and solution chemistry the following conclusions are drawn:

(1) Single-mineral flotation tests show that sodium silicate exhibits a certain depression on scheelite, which is consistent with Han's (Han et al., 2017) research results. Different addition orders of  $Mn^{2+}$  show different effects on the flotation behavior of scheelite. Adding  $Mn^{2+}$  before sodium silicate is not conducive for the flotation of scheelite.  $Mn^{2+}$  added after sodium silicate in order may activate the flotation of scheelite.

(2) The FTIR analysis indicated that the addition of  $Mn^{2+}$  could enhance the adsorption of NaOL

(Wang, et al. 2019).

(3) The results of the XPS analysis indicated that in the scheelite +  $Mn^{2+}$  + sodium silicate + NaOL flotation system, more hydrophilic silicate substances are formed, and these substances cover the surface of scheelite, hinder the adsorption of NaOL, and depress the flotation of scheelite. On the other hand, in the scheelite + sodium silicate +  $Mn^{2+}$  + NaOL flotation system,  $Mn^{2+}$  is adsorbed on the surface of scheelite treated by sodium silicate, which increases the cationic active sites on the surface of scheelite, enhances the adsorption of oleic acid ions on the surface of scheelite, and activates the flotation of scheelite.

(4) The chemical analysis of the solution revealed that manganese was primarily adsorbed on the surface of scheelite in the form of  $Mn^{2+}$  and  $Mn(OH)^+$ . The results of the thermodynamic analysis showed that, the  $\Delta G_{Mn^{2+}}^{\theta}$  is found to be negative in the pH range of 2–14, indicating that the reaction between NaOL and  $Mn^{2+}$  occurs spontaneously.

### Acknowledgments

This work was financially supported by the National Natural Science Foundation of China (No. 51504108, 51404119 and 51604130).

### References

- CHENG, L., FENG, Q., ZHAN, G., WEI, C., CHEN, Y., 2016. *Effect of depressants in the selective flotation of scheelite and calcite using oxidized paraffin soap as collector*. J International Journal of Mineral Processing 157:210-215.
- CHEN, W., FENG, Q., ZHANG, G., YANG, Q., ZHANG, C., XU, F., 2017. *The flotation separation of scheelite from calcite and fluorite using dextran sulfate sodium as depressant*, J. Miner. Process, 169, 53–59.
- CHEN, W., FENG, Q., ZHANG, G., YANG, Q., 2018. *Investigations on flotation separation of scheelite from calcite by using a novel depressant: Sodium phytate*. J Minerals Engineering 126:116-122.
- CHEN, R., 2019. *The influence of ionic wolframite flotation is unavoidable [D]*. Kunming University of Science and Technology.
- DENG, R., YANG, X., YUAN, H., KU, J., ZUO, W., MA, Y., 2018. *Effect of Fe(II) as assistant depressant on flotation separation of scheelite from calcite*. J Minerals Engineering 118:133-140.
- DONG, L., JIAO, F., QIN, W., LIU, W., 2019. *Selective flotation of scheelite from calcite using xanthan gum as depressant*. J Minerals Engineering 138:14-23.
- DONG, L., JIAO, F., QIN, W., LIU, W., 2019. *Effect of calcium ions on scheelite flotation using mixed collectors*. J Separation Science Technology 54(1):153-162.
- DONG, L., JIAO, F., QIN, W., LIU, W., ZHU, H., JIA, W., 2019. *Selective depressive effect of sodium fluorosilicate on calcite during scheelite flotation*. Minerals Engineering 131, 262–271.
- ESPIRITU, E.R.L., NASERI, S., WATERS, K.E., 2018. *Surface chemistry and flotation behavior of dolomite, monazite and bastnäsite in the presence of benzohydroxamate, sodium oleate and phosphoric acid ester collectors*. J Colloids Surfaces A: Physicochemical Engineering Aspects 546:254-265.
- FENG, B., LUO, X., WANG, J., WANG, P., 2015. *The flotation separation of scheelite from calcite using acidified sodium silicate as depressant*. Minerals Engineering 80:45-49.
- FENG, B., GUO, W., XU, H., PENG, J., LUO, X., ZHU, X., 2016. *The combined effect of lead ion and sodium silicate in the flotation separation of scheelite from calcite*. Separation Science 52(3):567-573.
- FLIPPOVA, I.V., FILIPPOV, L.O., LAFHAJ, Z., BARRES, O., DANIEL, F., 2018. *Effect of calcium minerals reactivity on fatty acids adsorption and flotation*. J Colloids Surfaces A Physicochemical Engineering Aspects 545:157-166.
- GAO, Y., GAO, Z., SUN, W., HU, Y., 2016. *Selective flotation of scheelite from calcite: A novel reagent scheme*. J International Journal of Mineral Processing 154(154):10-15.
- GAO, Z., SUN, W., HU, Y., 2015. *New insights into the dodecylamine adsorption on scheelite and calcite: An adsorption model*. J Minerals Engineering 79:54-61.
- HAN, H., HU, Y., SUN, W., LI, D., CAO, C., LIU, R., YUE, T., MENG, X., GUO, Y., WANG, J., GAO, Z., CHEN, P., HUANG, W., LIU, J., XIE, J., CHEN, Y., 2017. *Fatty acid flotation versus BHA flotation of tungsten minerals and their performance in flotation practice*. International Journal of Mineral Processing. 159, 22-29.
- HU, Y., GAO, Z., SUN, W., 2012. *Anisotropic surface energies and adsorption behaviors of scheelite crystal*. J Colloids Surfaces A Physicochemical Engineering Aspects 415(48):439-448.

- IGNATKINA, V. A., 2017. *Experimental investigation of change in the contrast between flotation properties of calcic minerals*. J Journal of Mining Science 53(5):897-906.
- KUPKA, N., RUDOLPH, M., 2018. *Froth flotation of scheelite – A review*. International Journal of Mining Science Technology 28(3): 373-384.
- LI, C., LU, Y., 1983. *Selective flotation of scheelite from calcium minerals with sodium oleate as a collector and phosphates as modifiers. II. The mechanism of the interaction between phosphate modifiers and minerals*. J International Journal of Mineral Processing 10(3):219-235.
- LI, Y., LI, C., 1983. *Selective flotation of scheelite from calcium minerals with sodium oleate as a collector and phosphates as modifiers. I. Selective flotation of scheelite Int. J Miner. Process.*, 10(3), 205-218.
- MARINAKIS, K.I., SHERGOLD, H.L., 1985. *Influence of sodium silicate addition on the adsorption of oleic acid by fluorite, calcite and barite*. J International Journal of Mineral Processing 14(3):177-193.
- SUN, W., TANG, H., CHEN, C., 2013. *Solution chemistry behavior of sodium silicate in flotation of fluorite and scheelite*. J Chinese Journal of Nonferrous Metals 23(8):2274-2283.
- SUN, W., WANG, R., HU, Y., HAN, H., 2018. *Activation and new theory of lead ion in minerals flotation process*. J Nonferrous Metals (Mineral Processing Section), 70(2): 91–98.
- TIAN, M., LIU, R., GAO, Z., CHEN, P., HAN, H., L, WANG., ZHANG, C., SUN, W., HU, Y., 2018. *Activation mechanism of Fe (III) ions in cassiterite flotation with benzohydroxamic acid collector*. J Minerals Engineering 119:31-37.
- WANG, J., BAI, J., YIN, W., LIANG, X., 2018. *Flotation separation of scheelite from calcite using carboxyl methyl cellulose as depressant*. J Minerals Engineering, 127, 329-333.
- WANG, J., MAO, Y., CHENG, Y., XIAO, Y., ZHANG, Y., BAI, J., 2019. *Effect of Pb(II) on the flotation behavior of scheelite using sodium oleate as collector*. J Minerals Engineering, 136, 161-167
- WANG, Z., WU, H., XU, Y., SHU, K., Yang, J., LUO, L., XU, L. 2020. *Effect of dissolved fluorite and barite species on the flotation and adsorption behavior of bastnaesite*. Separation and Purification Technology, 237, 116387.
- WANG, Z., WU, H., XU, Y., SHU, K., Yang, J., LUO, L., XU, L. 2020. *The effect of dissolved calcite species on the flotation of bastnaesite using sodium oleate*. Minerals Engineering, 145, 106095.
- WEI, Z., SUN, W., HAN, H., CAO, J., GUI, X., XING, Y., ZHANG, C., ZOU, J., 2020. *Enhanced electronic effect improves the collecting efficiency of benzohydroxamic acid for scheelite flotation*. Minerals Engineering, 152, 106308.
- YANG, S., PENG, T., LI, H., FENG, Q., QIU, X., 2015. *Flotation mechanism of wolframite with varied components Fe/Mn*. Mineral Processing & Extractive Metallurgy Review, 37:1, 34-41.
- YAO, W., LI, M., ZHANG, M., CUI, R., SHI, J., NING, J., 2020. *Decoupling the effects of solid and liquid phases in a Pb-water glass mixture on the selective flotation separation of scheelite from calcite*. Minerals Engineering, 154, 106423.
- YIN, W., WANG, J., 2014. *Effects of particle size and particle interactions on scheelite flotation*. J Transactions of Nonferrous Metals Society of China 24(11):3682-3687.
- ZHANG, Y., LI, Y., CHEN, R., WANG, Y., DENG, J., LUO, X., 2017. *Flotation separation of scheelite from fluorite using sodium polyacrylate as inhibitor*. J Minerals, 7(6):102.
- ZHANG, Y., HU, Y., WANG, Y., WEN, S., 2014. *Effects of sodium silicate on flotation behavior of calcium-bearing minerals and its mechanism*. J Chinese Journal of Nonferrous Metals 24(9):2366-2372.
- ZHAO, G., WANG, S., ZHONG, H., 2015. *Study on the Activation of Scheelite and Wolframite by Lead Nitrate*. J Minerals 5(2):247-258.
- ZHAO, W., HU, Y., HAN, H., SUN, W., WANG, R., WANG, J., 2018. *Selective flotation of scheelite from calcite using Al-Na<sub>2</sub>SiO<sub>3</sub> polymer as depressant and Pb-BHA complexes as collector*. J Minerals Engineering 80, 45-49.
- ZHANG, Z., CAO, Y., MA, Z., LIAO, Y., 2019. *Impact of calcium and gypsum on separation of scheelite from fluorite using sodium silicate as depressant*. Separation and Purification Technology, 215, 249–258.